Fiber-optic tram vehicle detector

JAN NEDOMA[a,*], MARCEL FAJKUS[a], STANISLAV ZABKA[a], RADEK MARTINEK[b]
aDepartment of Telecommunications, Faculty of Electrical Engineering and Computer Science,
VSB - Technical University of Ostrava, 17 Listopadu 15/2172, 708 33 Ostrava, Czech Republic
bDepartment of Cybernetics and Biomedical Engineering, Faculty f Electrical Engineering and Computer
Science, VSB - Technical University of Ostrava, 17 Listopadu 15/2172, 708 33 Ostrava, Czech Republic

This article describes a compact trackside low-cost measuring sensor with basic advantages such as immunity to electromagnetic interference and ability to remotely evaluate information (the tested distance was 3000 m). The proposed sensor is constructed to detect vibration-acoustic responses caused by tram vehicles. The sensor was tested in real tram traffic. Over a period of six months, a total of 1435 tram vehicles were recorded (different types of tram vehicles) with 100 % detection success. The massive expansion of optical cables along the railways provides our system could be directly connected to as well as being remotely monitored and evaluated.

1. Introduction

In this article, we discussed and described a type of fiber-optic interferometric sensor based on the Michelson interferometer. The basic reason why we focused on the fiber-optic sensor is its immunity to electromagnetic interference (EMI). Currently used electrical and electromagnetic sensors have problems with their functional reliability. The primary reason for this reduction is the new traction drives of tram and train vehicles that generate electromagnetic interferences, as well as the signal contamination caused by the return traction current in rails [1-2]. A very important problem of electrical detection systems is their low resistance to influences or damage caused by atmospheric discharge. With facilities with metallic interconnections, undesirable conductive loops get closed through these electrically conductive circuits and their treatment against undesirable influences and damage is very difficult. With the proposed interferometric sensor, the mentioned problems can be eliminated.

The range of maximum amplitudes and frequencies (which rail and tram vehicles can generate) is defined in International Standard ISO 4866:2010 [3]. This standard defines a frequency range of 1-80 Hz (practically ranging from 20-50 Hz); our interferometric sensor is designed to exhibit the highest sensitivity in the range of the above-mentioned frequencies according to International Standard ISO 4866: 2010.

Detection principle is as follows. Passage a railway vehicle around a sensor is caused above-mentioned frequency response (ω) practically ranging from the 20-50 Hz. This vibration and acoustic response excite the measurement fiber of the interferometric sensor and causes a change in its optical length or more precisely the product of its refractive index *n* and geometric length *L*. The resulting phase change $\Delta\phi$ is given by the phase changes of the light source ($\delta\phi_1$) as well as the changes in the length of the arm and its refractive index ($\delta\phi_2$). The phase changes of the source ($\delta\phi_1$) will occur in both arms of the interferometric sensor (reference and measurement arms) and one will be subtracted from the other, while the phase changes due to a vibration source ($\delta\phi_2$) that carry information about measured frequencies (ω) caused by the passage of a railway vehicle only occur in the measurement arm of the interferometric sensor.

Contemporary sensors for detecting rail vehicles can be divided into two basic categories: 1) conventional sensors; 2) fiber-optic and optical sensors.

1.1. Conventional sensors

For railway transport, the sensor types described below are either in practical use or have been experimentally tested. Currently, to monitor whether a track is occupied or not, track circuits are typically used. This technology operates on a principle that senses when a track (or railway) is split into pre-determined parts and electrically isolated. The passing train causes the circuit between two fixed spots (rails) to close, and this leads to the detection of the train [4-6]. An alternative solution is based on wheel detectors or axle counters, which use the flange to mechanically connect several contacts. By this means, the train as well as its speed and direction can be detected [7-9]. The Light Detection and Ranging (LIDAR) Technology (installed close to the railway) has been used for the monitoring of quantities such as: the presence of a train, the train's speed, the curvature of the tracks, etc. For the measurement and determination of the required parameter, the pulse scattering time of a laser radiation source from the analyzed object is used [10-11]. The

European Train Control System (ETCS) is a current conventional system. The track part of the system consists of several parts, particularly Eurobalise, Lineside Electronic Unit (LEU), Euroloop, Radio Block Center (RB), and an additional radio in-fill unit. The basic monitoring element is Eurobalise, which transmits information to the train. The device itself is powered during the passage of a train [12-13].

1.2. Fiber-optic interferometric sensors

The use of interferometric sensors is further described in articles [14-15]. The authors of [14] reflect on the use of an acoustic fiber-optic sensor for the monitoring of a railway infrastructure from a long distance on the basis of an interferometric connection. They explain that each acoustic activity caused by the reflection from a railway vehicle is recorded by a sensitive sensor and processed with the use of an evaluation unit. It is therefore possible to record the passage of the train as well as its speed with two sensors. Article [15] describes the implementation of optical sensors on the basis of the Fabry-Perot Interferometer during the production to the pre-stressed pre-fabricated sleepers made of concrete and steel, which are supported by a concrete or asphalt structure. These sensors can be used to calculate the number of axles and the direction, as well as the train's speed with more sensors. However, their installation in sleepers is necessary. In the patent described in [16], an interferometric sensor is used for the detection of railway vehicles and for the calculation of the number of axles, i.e. an axle counter. The principle of the detection used in this patent is based on scanning the vibration response during the passage of a train. To apply this sensor, it is necessary to place its sensing element in direct physical contact with the rails. The reference element including its evaluation part is then placed away from the rails. In patent [17], there is a description of the basic principle of a railway vehicle axle counter based on a fiber-optic interferometer. The sensing element of the optical fiber of the interferometer is physically attached to the rail and a multimode optical fiber is included in the railhead. A change in the geometry of the optical fiber as a result of exerting pressure on the fiber due to the passage of the railway vehicle changes the Speckle images of the measuring fiber. An alternative track vibration monitoring system based on the two-arm Mach-Zehnder interferometer [18] has been proposed, demonstrated and tested along a single railway track in the Prague subway system. Two passive detection systems placed 50 m and 1.3 km away from the control room were used to measure tunnel vibrations triggered by passing trains free from the effect of any unrelated EMI existing in the subway tunnel. In article [19], authors proposed a fiber-optic system consisting of one or more passive fiber trackside sensors based on the three arm Mach-Zehnder interferometer, and an x86 processing unit located at the work site. The system was tested in real traffic with the results obtained indicating the successful detection of all the rail vehicles with one sensor.

The main contribution of this article is verification of the compact track-side sensor based on the Michelson interferometer, which, thanks to the high sensitivity, enables non-destructive installation and monitoring of selected rail parameters.

2. Methods

The experimental results presented in our work are based on a two-armed Michelson interferometer. The optical phase delay of light passing through a fiber is given by the following equation (1):

$$\Phi = nLk, \tag{1}$$

where k is an optical wavenumber in vacuum (can also be expressed as $2\pi/\lambda$), λ is the wavelength of the light source, L is the physical length of the used optical fiber and n is the refractive index of the fiber core.

The definition of interference visibility is given by the following equation (2):

$$V = \frac{\sqrt{\alpha_r \, \alpha_s c_1 c_2 (1-c_1)(1-c_2)}}{\alpha_r \, c_1 c_2 + \alpha_s \, (1-c_1)(1-c_2)}, \tag{2}$$

where c_1 and c_2 are coupling coefficients, and a certain optical loss in the measuring and reference arm can be assumed, known as α_s and α_r. The output intensity of the used Michelson interferometer can be given by the following equation (3):

$$I = \frac{I_0 \, \alpha}{2} (1 + cos \, \Delta_\Phi), \tag{3}$$

where $\Delta_\Phi = (\Phi_r - \Phi_s)$ is the phase difference between the reference (Φ_r) and sensoric (Φ_s) arm of the used interferometer. Parameter α represents losses on the interferometer and parameter I_0 characterizes the mean signal value. The output of used detector creates an electrical current (the measured signal of tram vehicles) and can be given by the following equation (4):

$$i = \varepsilon \cdot I_0.\alpha \cdot cos \, (\phi_d + \phi_e \cdot \sin \omega t), \tag{4}$$

where ε is the sensitivity of the photodetector, I_0 is the mean signal value, ϕ_d represents the changing phase shift, ϕ_e is the duration of the amplitude, and ω symbolizes the frequencies applied to the interferometer, i.e. its measurement arm [20-21].

A simplified scheme of the fiber-optic Michelson interferometer used in our work is shown in Fig. 1. Fig. 1 used a DFB (Distributed Feedback) laser with the reference output power of 1 mW. DFB laser works with a wavelength of 1550 nm and a spectral line width of 0.03 nm. Photodetector (PD) PbSe (Polycrystalline lead Selenide) was used as an optical receiver. An optical isolator (IR fiber Optic Isolators with SM fiber) allows the transmission of light in only one direction. An optical

circulator is a three-port device that allows light to travel in only one direction (type SM Optical Circulators, 1550 nm, FC/APC). The signal from the laser is divided by optical coupler (type SM 1550 nm with coupling ratio 1:1). The arms of Michelson interferometer were formed by 1 m long fibers (SMF, ITU-T. G.652.D) and terminated with mirrors. Used fiber-optic mirrors reflect lights directly back, with low optical losses (<1 dB). The presented sensor unit is completely based on the single-mode optical fiber (SMF, ITU-T. G.652.D).
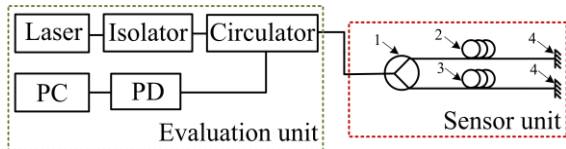
Fig. 1. Simplified scheme of the fiber-optic Michelson interferometer (1 – Optical coupler; 2 – Measuring arm; 3 – Reference arm; 4 – Mirrors)

2.1. Signal processing

The conversion to the measuring electrical current (by photodetector) is followed by further signal processing. The simplified block diagram that consists of several parts is shown in Fig. 2.
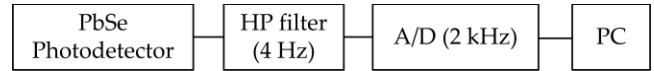
Fig. 2. A simplified block diagram of the signal processing

The signal processing scheme consists of an HP (High Pass) filter with a cutoff frequency of $f_0 = 4$ Hz, analog-digital converter (A/D) in the form NI myDAQ Card with sampling frequency 2 kHz and computer (PC) unit with LabVIEW software (2015, National Instruments, Austin, Texas, USA). The utilization of an analog filter (HP) before the A/D converter (NI myDAQ card) seems to be an optimal option, because it improves the dynamic range of the measurement and practically leads to the removal of the DC (direct current) component, which is caused by the instability of the light polarization and external influences (the temperature). The algorithm for processing the passing tram vehicles around the interferometric sensor unit was written in the above-mentioned LabVIEW environment. The maximum intensity of the measured signal is reached when the tram vehicles are at the sensor unit level. The algorithm compares the useful signal (caused by the first axle of the passing tram vehicles) against noise background (caused by the environment around the sensor unit). Based on the experimental measurements, the level (min. 3 dB) between useful signal and noise background was set up so that if the signal level meets this condition, the algorithm evaluates it as the vehicle's passage. For better clarity, the screen of the monitoring application is shown in Fig. 3.
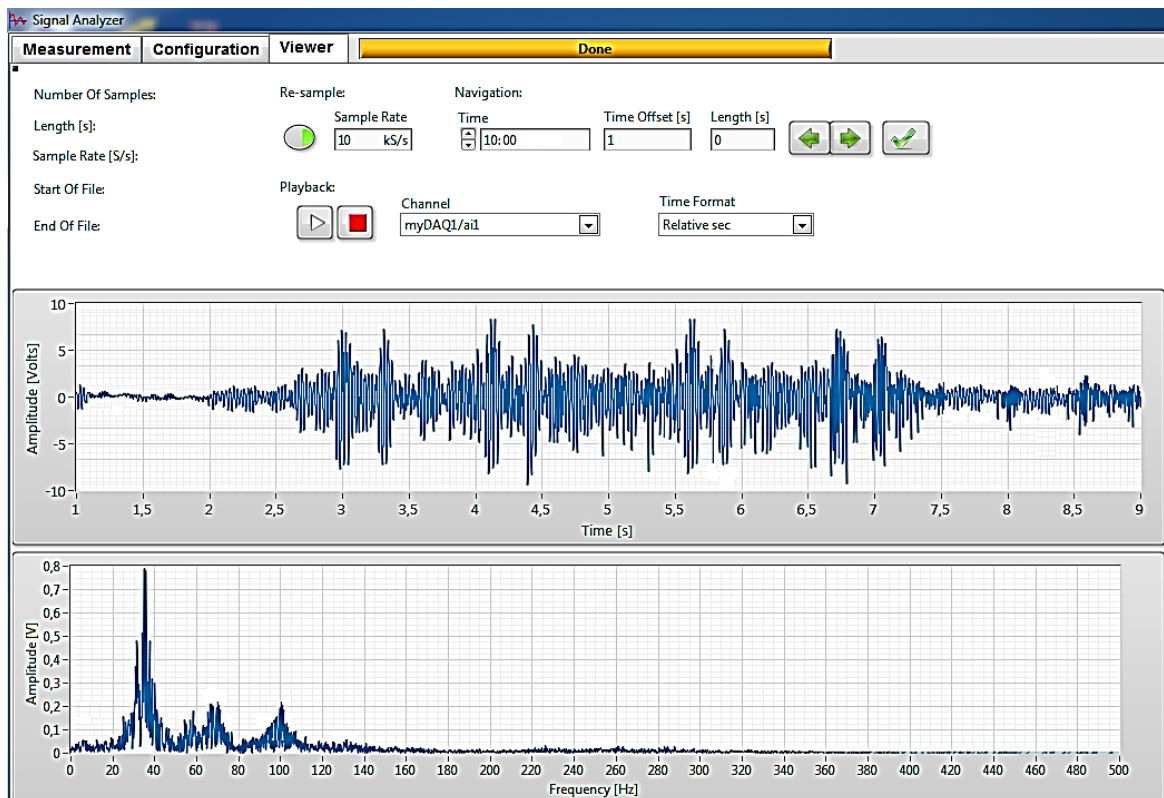
Fig. 3. Screen of the monitoring application

A photo of the real sensor unit is shown in Fig. 4. The input-output interface is created by the FC/APC connector (red marked in Fig. 4). The interferometric sensor is stored in a waterproof box, the resonant frequency of the plastic box lies outside the range of the measured frequencies. The dimensions of a waterproof plastic box are 40:30:12 cm (height:width:depth). The internal arrangement of the sensor is divided into two parts - measuring and reference. The reference part contains the reference arm of the Michelson interferometer and optical coupler. The reference part is based on acoustic foam with a 3 cm thickness. The acoustic foam was chosen based on previous research of our team, please see publications [22-23]. The measuring part contains the measuring arm of the Michelson interferometer; this arm is stored circularly. The methodology of fiber storing and selection of cover materials was chosen based on our previous research, please see publications [24-25].
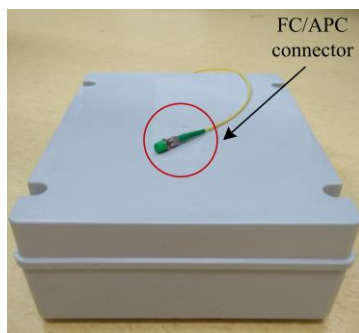
Fig. 4. Real photo of the sensor unit

Fig. 5 shows the analysed frequency characteristic of the interferometric sensor. The highest sensitivity is achieved in the range of 4 to 85 Hz according to ISO standard 4866:2010.
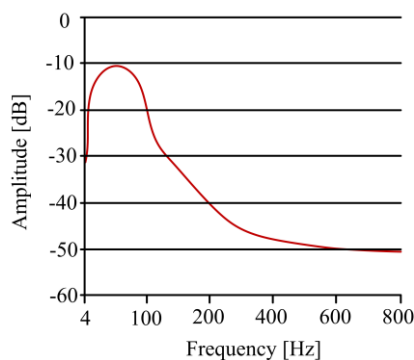
Fig. 5. Frequency spectrum of the interferometric sensor

3. Experimental setup and results

This section contains the measured results, their statistical processing and graphic illustrations of time and frequency records analyzed for the tram passages by an interferometric sensor, which are based on 1.435 measurements. Performed experimental measurements took place over the course of 6 months in total, or during 16 measuring days (from November to January and from June to August), so the functioning of the sensor was tested in different climatic conditions. The measurements took place at three different places in Ostrava (1. Podzámčí Street - GPS coordinates 49.8293328N, 18.2975139E, 2. U Haldy Street - GPS coordinates 49.7879486N, 18.2706658E, 3. Dr. Martinka Street - GPS coordinates 49.7871106N, 18.2690781E). Various types of trams were tested/recorded (4 types in total; Vario LFR, ČKD T3, Inekon LTM 10.08 and Inekon 2001 TRIO). The range of the speeds of trams was between 10 and 70 kph according to speed limits on routes given by traffic, but the most between the range 50-70 kph. The distance of any sensor or sensor system from the rails is defined by the hazardous area of traction lines according to standard CSN 34 1500 ed. 2 from 2011 in the Czech Republic [26]. This standard defines the space of 3 m in each direction from the rail pad. A sensor was placed at a distance of 3 m from the rail pad in all three measured locations. There were two-lane rails at all 3 mentioned locations (in the direction / in the opposite direction). The results given below also contain the results of the tram detection in the opposite direction. A measurement diagram can be seen in Fig. 6. As a reference we used a camera system.
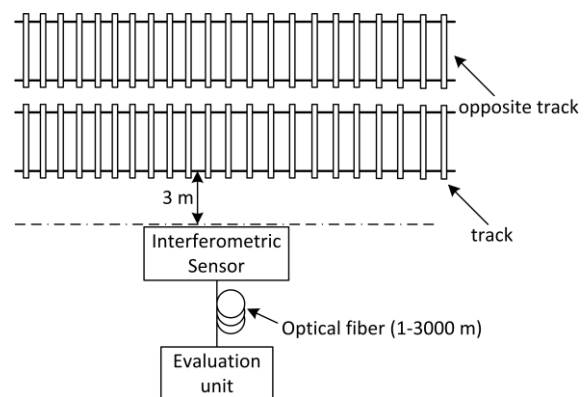
Fig. 6. The diagram is valid for the 3 mentioned locations

Fig. 7 includes a photograph capturing the placement of the sensor at a distance of 3 m from the rail pad at the practical measurement in the Podzámčí street.

Fig. 7. A photo from the real measurement (red marked position of the interferometric sensor)

Figs. 8 and 9 depict an example of a time record and Fig. 10 depict an example of a frequency record for the tram passage (type ČKD T3 tram) made in the Czech Republic, which has the total of 2 wagons.
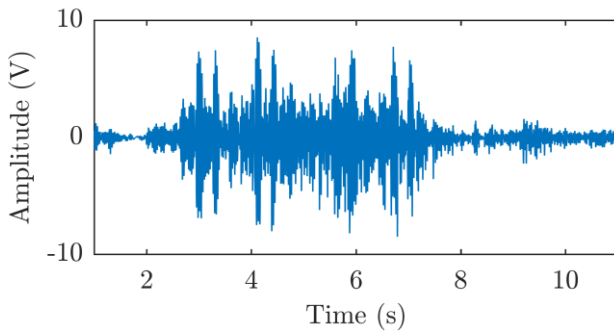
Fig. 8. Example of a time response caused by a tram passage (type ČKD T3)
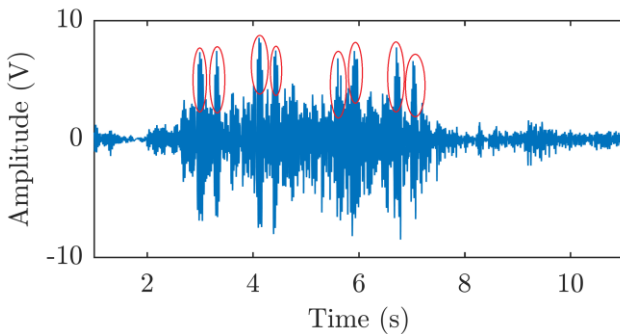
Fig. 9. Example of a time response caused by a tram passage (type ČKD T3); Red marked the individual detected maxima which characterize the number of axles

In Fig. 8 and 9, the x axis shows the time [s] and the y axis shows the amplitude [V], which corresponds to the resulting intensity of optical radiation falling on the photodetector and is adequate to the phase change between the light beams spread through the arms of the interferometers.

It is also possible to see the individual maximums (red in Fig. 9) that characterize the number of axles (ČKD T3 tram has 4 axles, i.e. all 8 detected axles for 2 wagons of the tram are visible there).
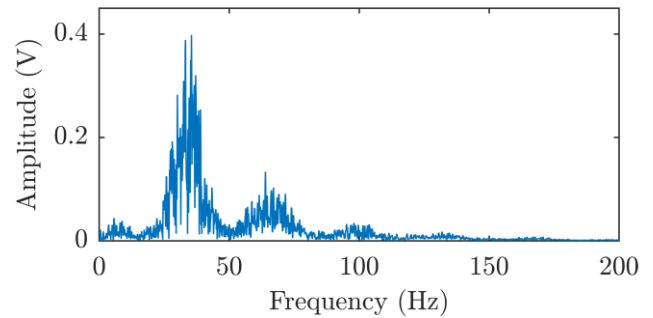
Fig. 10. Example of a frequency response caused by tram passage (type ČKD T3)

In Fig. 10, the x axis shows the frequency [Hz] and the y axis shows the amplitude [V], see the text above at the description of Fig. 8 and 9.

The summary of the measured results is depicted in Table 1. Table 1 clearly shows that in all 16 measuring days all types of trams were recorded. The results also show that a negative influence of various climatic conditions on the effectiveness of the sensor or the measuring system was not recorded. It was also confirmed that no negative influence on the effectiveness of the sensor due to various speeds, weight or the number of wagons of individual trams was recorded. It is also obvious that the sensor is so sensitive that even trams in the opposite direction were detected.

Table 1. Summary of the measured results

Measuring day	Time period	Number of passages (in the direction / in the opposite direction)	Detection success rate (%)
1		52/41	100/100
2		42/44	100/100
3	November December January	47/46	100/100
4		39/42	100/100
5		45/43	100/100
6		51/48	100/100
7		38/41	100/100
8		44/46	100/100
9		42/44	100/100
10		44/45	100/100
11	June July August	47/44	100/100
12		42/48	100/100
13		39/41	100/100
14		47/44	100/100
15		49/51	100/100
16		52/47	100/100

4. Discussion

The detection of axles of railway vehicles using interferometric sensors was described in publications [15-17] that are listed in the beginning of this publication. All of the above described detection methods are dependent on the direct connection of a sensor (a measuring arm) to a rail. The sensor described in this publication doesn't have

to be connected to the rail (it was tested at a distance of 3 m from the rail pad) and the axles can be monitored reliably.

The maximum distance between the sensor and the evaluation unit (3000 m) was tested using a single-mode cable (SMF, ITU-T. G.652.D). The input power was increased to 3 mW. An input power of the radiation source of 1 mW was sufficient up to a distance of 500 m (sensor – evaluation unit).

The basis of this sensor is immunity to electromagnetic interference (EMI) and simple implementation because the sensor does not need to be installed destructively on the rails. Due to the massive expansion of optical cables along roads and railways that secure telecommunications and security services, there is an important advantage in the possibility of the direct connection of the sensor to the existing infrastructure and remote evaluation.

Because we used only one sensor, we did not focus during the experiment on the speed of the tram vehicles. Also, we primarily focused only on satisfactory detection of trams, because our research is on the beginning.

The possibility of how we can calculate the speed is using the time-marks caused by the individual axles (If we know the distance of the axles). However, unfortunately, during the experiments, we did not record the speed of tram vehicles, so we do not have the appropriate reference and we can not reliably determine with what accuracy the speed can be analysed. Our next step of research will more focus on further traffic parameters such as speed.

When there are two trains pass by at the same time, the sensor or system can provide an accurate detection using the frequency analysis. Individual tram kits differ primarily in their frequency response and their typical frequency responses. In only three cases (when two train passes at the same time), we noticed overlapping spectra, so we were not able to recognize the individual trams using the frequency analysis. This could be solved by using two sensors (each sensor for a separate track).

Based on the presented results the follow-up research measurements of underground railway system detection were performed in real operation in the Prague underground tunnels between: I. P. Pavlova – Vysehrad. The measurements will be performed upon agreement and after training by Prague's transport company. Fig. 11 shows a photo of the installation of the sensor. The results of the measurements will be discussed in the following publication.

Fig. 11. Photo of the real installation in Prague Underground

5. Conclusion

Interferometric sensor systems offer a potential for rail transport thanks to their high sensitivity. The proposed and described system was tested over the course of 6 months in real tram operation. The statistical evaluation is based on a total of 1.435 passages of a tram, which were detected with a 100 % success rate. The operation of the system is trouble-free, it can be easily implemented, and the information can be evaluated from a distance (practically was tested 3000 m). Further research will focus on minimizing the sensor and practical experiments for train transport.

References

[1] M. N. Halgamuge, C. D. Abeyrathne, P. Mendis, Radiat. Prot. Dosimetry **14**(3), 255 (2010).
[2] D. Thompson, Railway Noise and Vibration, Elsevier Science 536 (2009).
[3] ISO4866:2010 [Available] https://www.iso.org/ standard/38967.html.
[4] J. Marshall, North Pomfret, Vt.: David, (1978).
[5] J. Chen, C. Roberts, P. Weston, Control Engineering Practice **16**(5), 585 (2008).
[6] Dealing with a train accident or train evacuation (Module M1), Iss. 4, RSSB, (2015).
[7] J. C. O. Nielsen, A. Johansson, Proceedings of the Institution of Mechanical Engineers, Part F: Journal of Rail and Rapid Transit **214**(2), 79 (2005).
[8] A. K. S. Jardine, D. Lin, D. Banjevic, Mechanical Systems and Signal Processing **20**(7), 1483 (2006).
[9] R. W. Ngigi, C. Pislaru, A. Ball, F. Gu, Journal of Physics: Conference Series **364**, s. 012016 (2012).
[10] Y. Jwa, G. Sohn, ISPRS Annals of Photogrammetry, Remote Sensing and Spatial Information Sciences **II-**

3/W5, 159 (2015).

[11] M. Leslar, P. Gordon, K. Mcnease, ASPRS 2010 Annual Conference, San Diego, (2010).

[12] Marco Biagi, Laura Carnevali, Marco Paolieri, Enrico Vicario, Transportation Research Part C: Emerging Technologies **82**, 314 (2017).

[13] T. Babczyński, J. Magott, Advances in Intelligent Systems and Computing **286**, 37 (2014).

[14] E. Udd, W. Schulz, J. Seim, J. Corones, H. M. Laylor, Fiber optic Sensors for infrastructure applications (Final report), (1998).

[15] S. Crail, D. Reichel, U. Schreiner et al., SPIE Proceedings **4694**, 259 (2002).

[16] Rail contacting device in railway systems, particularly for axle counting devices, DE 3537588 A1.

[17] A. G. Blednin, Contact fiber optic impact sensor, Patent, US6144790 A.

[18] S. Kepak, J. Cubik, P. Zavodny, P. Siska, A. Davidson, I. Glesk, V. Vasinek, Optical and Quantum Electronics **48**(7), art. no. 354 (2016).

[19] S. Kepak, J. Cubik, P. Zavodny, S. Hejduk, J. Nedoma, A. Davidson, V. Vasinek, Proceedings of SPIE - The International Society for Optical Engineering **10142**, art. no. 101421M (2016).

[20] M. Born, E. Wolf, Principles of Optics: electromagnetic theory of propagation, interference and diffraction of light, 7th ed. New York: Cambridge University Press, (1999).

[21] E. Wolf, Introduction to the theory of coherence and polarization of light, Cambridge: Cambridge University Press (2007).

[22] J. Nedoma, M. Fajkus, R. Martinek, L. Bednarek, S. Zabka, D. Hruby, J. Jaros, V. Vasinek, Proceedings of SPIE - The International Society for Optical Engineering **10208**, art. no. 102080V (2017).

[23] J. Nedoma, M. Fajkus, R. Martinek, O. Zboril, L. Bednarek, M. Novak, K. Witas, V. Vasinek, Proceedings of SPIE - The International Society for Optical Engineering **10231**, art. no. 1023119 (2017).

[24] J. Nedoma, M. Fajkus, V. Vasinek, Proceedings of SPIE - The International Society for Optical Engineering **9994**, art. no. 99940P (2016).

[25] J. Cubik, S. Kepak, M. Fajkus, O. Zboril, J. Nedoma, A. Davidson, V. Vasinek, Proceedings of SPIE - The International Society for Optical Engineering **10142**, art. no. 101421A (2016).

[26] ČSN 34 1500 ED.2 (341500) - Drážní zařízení – Pevná trakční zařízení - Předpisy pro elektrická trakční zařízení [Available] http://www.technicke-normy-csn.cz/341500-csn-34-1500-ed-2_4_84547.html.

_____
*Corresponding author: jan.nedoma@vsb.cz